

Valley splitting control in SiO₂/Si/SiO₂ quantum wells in the quantum Hall regime

K. Takashina, A. Fujiwara, S. Horiguchi,* and Y. Takahashi

NTT Basic Research Laboratories, NTT Corporation, 3-1 Morinosato Wakamiya, Atsugi-shi, Kanagawa 243-0198, Japan

Y. Hirayama

*NTT Basic Research Laboratories, NTT Corporation, 3-1 Morinosato Wakamiya, Atsugi-shi, Kanagawa 243-0198, Japan
and SORST-JST, 4-1-8 Honmachi, Kawaguchi-shi, Saitama 331-0012, Japan*

(Received 12 January 2004; revised manuscript received 9 March 2004; published 15 April 2004)

SiO₂/Si/SiO₂ quantum wells fabricated on SIMOX silicon-on-insulator substrates are examined in the quantized Hall regime. An 8 nm quantum well behaves as a single layer of two-dimensional electrons at accessible gate voltages. By using front and back gates, the wave function in the confinement direction can be shifted continuously between two SiO₂/Si interfaces formed through different processes. We find that this results in a continuous evolution of the valley splitting which is asymmetric with electrical gate bias. Wider quantum wells show bilayer behavior where the valley splitting is different in each layer, demonstrating that its control shown by the 8 nm well arises due to the different properties of the two interfaces. Estimates of the valley splitting are made through Landau level coincidences and activation energies. The coincidence between Landau levels of opposite spin, opposite valley, and like cyclotron indices at $\nu=6$ shows anticrossing behavior.

DOI: 10.1103/PhysRevB.69.161304

PACS number(s): 73.40.Qv, 73.43.Fj, 73.63.Hs, 71.70.Di

The valley degree of freedom in valley-degenerate semiconductors such as Si and AlAs remains a subject of considerable attention despite its long history. This is first due to interest in the valley splitting lifting this degeneracy for which there is still no unified picture to describe its origin¹ and observations, such as its enhancement with magnetic field recently reported.^{2,3} Second, valleys offer an unexplored degree of freedom in relation to Landau level coincidences and quantum Hall ferromagnetism,⁴⁻⁶ where the valley index specifying the valley in \mathbf{k} space could be taken in analogy with the layer or subband index of a real-space bilayer system. Previous experiments in valley degenerate Si/SiGe have found striking phenomena at coincidences between Landau levels of opposite spin and differing cyclotron indices but the role of the valley degree of freedom is unknown.⁶ For the exploration of both these issues, it is highly desirable to be able to control the valley splitting.

In (100)-silicon metal-oxide-semiconductor field effect transistors (MOSFET's), which have two-fold valley degeneracy, it is relatively well established that the valley splitting changes with carrier concentration.¹ This is attributed to the change in confinement in the z direction which allows coupling between valleys separated in k_z . Accordingly, there have been demonstrations that the valley splitting can also be enhanced by the application of a substrate bias.^{7,8} However, there have been no successful attempts to exploit this control in examining interaction effects at level coincidences in the quantum Hall regime. In this paper, we present a system which allows the valley splitting to be tuned over a large energy range, by exploiting the differing properties of two interfaces forming a quantum well. A level coincidence at $\nu=6$ between Landau levels of opposite valleys and opposite spins is observed and is used to obtain estimates of the valley splitting. This coincidence is found to show anticrossing behavior.

We examine magnetotransport properties of two-dimensional electron gasses in silicon-on-insulator (SOI)

MOSFET's. A schematic diagram of the samples is shown in Fig. 1. A SIMOX (separation by implantation of oxygen),⁹⁻¹¹ SOI substrate is prepared by ion implantation of oxygen into a (100) silicon wafer followed by high-temperature annealing, leading to a buried layer of SiO₂ or BOX (buried oxide). Despite the initial continuous spatial distribution of implanted oxygen atoms, annealing at high temperature for a prolonged period of time is known to yield abrupt Si/SiO₂ interfaces and recrystallization of the implantation-damaged silicon. MOSFET's fabricated on these SOI substrates lead to SiO₂/Si/SiO₂ quantum wells where the BOX acts as an intrinsic back-gate insulator.

Previous low-temperature magnetotransport measurements of SIMOX MOSFET's with wide well widths¹² found that the Si/BOX interface was of sufficient quality to observe Shubnikov-de Haas oscillations but neither spin nor valley splitting could be resolved. Measurements by Ouisse *et al.*¹³ on ultrathin samples with width of order 3 nm fabricated by similar processes to ours found that Shubnikov-de Haas oscillations were hardly observable using the back gate alone. However, using a combination of front and back gates, they observed beating patterns in the oscillations which they attributed to a valley splitting which could be tuned between unusually large values of 5 and 20 meV by changing the back-gate bias. Individual quantized Hall states could not be observed in their samples presumably due to the narrow well

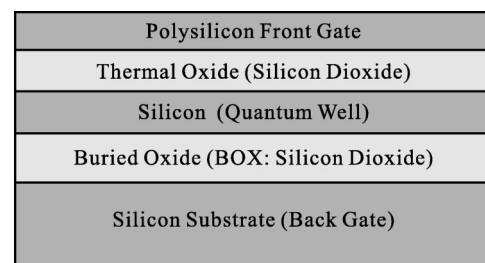


FIG. 1. A schematic diagram of the sample structure.

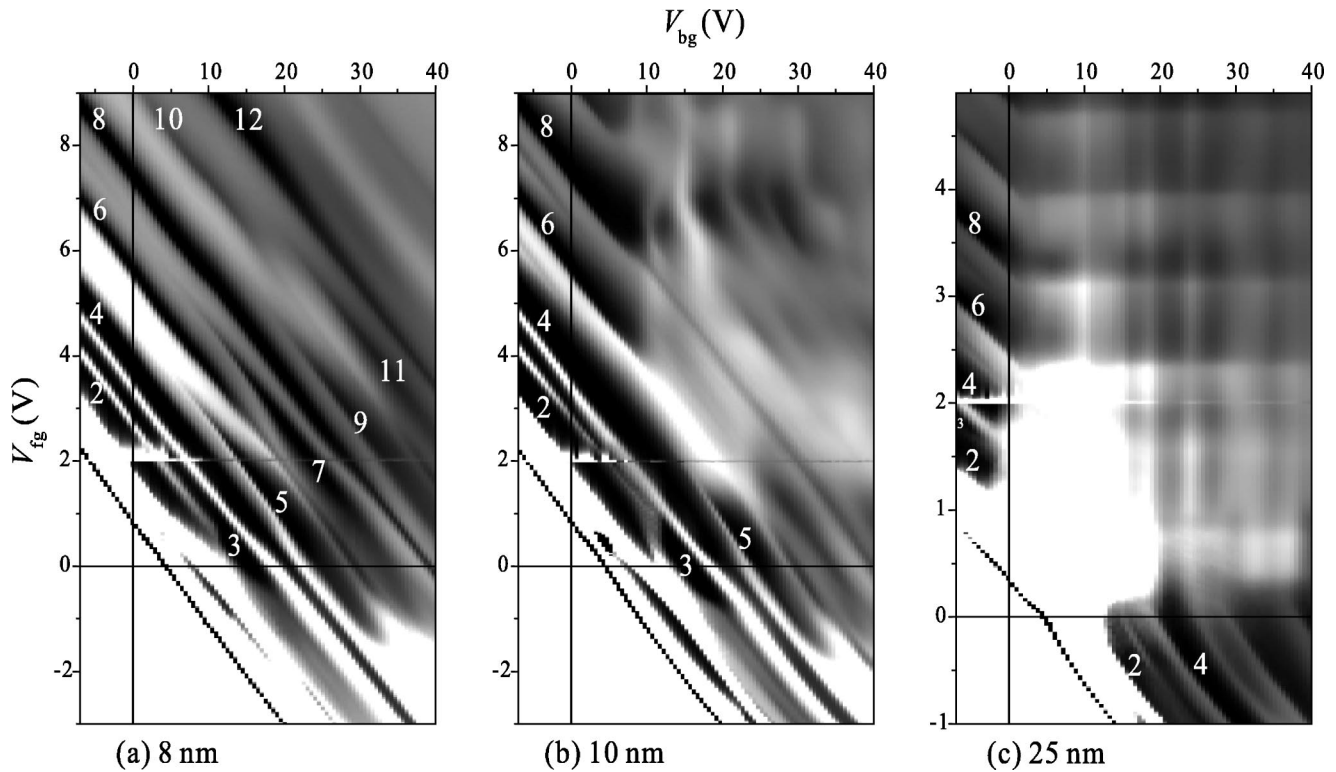


FIG. 2. Gray-scale plots of the longitudinal resistance at 350 mK, at a fixed value of magnetic field of 11 T as functions of front- and back-gate voltages. (a), (b), and (c) respectively, show data for samples with well-widths of 8, 10, and 25 nm. Dark regions correspond to quantized Hall states with vanishing longitudinal resistance. The figures represent the filling factors corresponding to the measured quantized Hall resistance. The white triangular regions on the bottom left of each graph represent regions in which the carrier concentration is too low for Ohmic contacts. The horizontal lines at $V_{fg}=2$ V are experimental artifacts.

width leading to large disorder broadening of the Landau levels. In this paper we present data, in the quantized Hall regime, directly showing the evolution of the valley splitting of individual Landau levels from a regime of conventional MOSFET's with small valley splitting to one where the valley splitting is strongly enhanced due to the Si/BOX interface.

Three samples were studied with different silicon well widths of 8, 10, and 25 nm. A rough indication of the quality of the samples can be obtained from the two interfaces in the 25 nm wide quantum well as we find the two electron layers in this sample to be rather independent. The front layer on the thermal oxide interface has a peak mobility of $1.0 \text{ m}^2/\text{V s}$ while the back layer on the BOX interface has a peak mobility of $0.4 \text{ m}^2/\text{V s}$ at 1.5 K.

Magnetotransport measurements were made using standard lock-in techniques on large Hall bar devices at 350 mK, the base temperature of a helium-3 cryostat. Gray-scale plots in Fig. 2 show longitudinal resistance data at 11 T as functions of the front- and back-gate voltages. Light regions correspond to high resistance while the dark regions correspond to situations where the resistance becomes vanishingly small due to the quantum Hall effect (QHE). The figures indicate the filling factor ν obtained from the values of the quantized Hall resistance (not shown).

When a positive voltage (V_{fg}) is applied to the front gate while the back-gate voltage (V_{bg}) is zero or at negative values, we expect the behavior to be similar to that found in

conventional MOSFET's. This is because the situation corresponds to one where the wave function is pressed against the top thermal-oxide-silicon interface which has been prepared by conventional methods. For each of the plots below $V_{bg}=0$ V, quantized Hall states at $\nu=4(n+1)$ can clearly be seen corresponding to cyclotron gaps where n ($=0,1,2, \dots$) is the cyclotron Landau-level index of the uppermost occupied Landau level. (For each cyclotron state n , there are two spin and two valley states.) Quantized Hall states can also be seen at $\nu=4n+2$ corresponding to spin gaps between two sets of valley degenerate Landau levels. For the lowest Landau level, the $\nu=3$ state can be seen for each of the samples corresponding to a valley gap. Resistance minima at higher odd integers are either missing or not very deep showing that the valley splitting is much smaller than the spin splitting.

Focusing our attention on data for the 8 nm wide sample between $\nu=4$ and 8, we see that as the back-gate voltage is increased to around $V_{bg}=13$ V, the resistance peaks dividing $\nu=4, 6$, and 8 split giving rise to odd filling quantum Hall states. At the same time, the spin-split QHE resistance minimum at $\nu=6$ becomes shallower. We interpret this as being due to an increase in the valley splitting Δ_V leading to the odd-integer quantum Hall states which in turn reduces the mobility gap for the spin-split $\nu=6$ state as schematically illustrated in Fig. 3.

With V_{bg} increased further, there is a saddle point in $R_{xx}(V_{bg}, V_{fg})$ at $\nu=6$ at $V_{bg}=20$ V beyond which the resis-

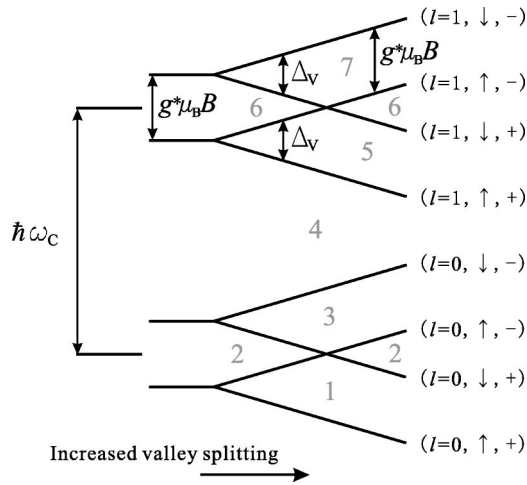


FIG. 3. A schematic diagram of Landau levels belonging to two lowest orbital states $l=0$ and $l=1$. The indices in brackets labeling the levels ($l, \uparrow/\downarrow, +/-$) represent the orbital Landau level, spin and valley indices, respectively. The gray numbers represent the filling factor when the Fermi energy lies in the corresponding gap.

tance minimum deepens again. At the same time, the cyclotron minima at $\nu=4$ and 8 become shallower. This is due to the continued increase in the valley splitting leading to a level crossing as depicted in Fig. 3. There is a level coincidence between Landau levels of the same cyclotron index, opposite spin, and opposite valleys. The fact that there is a saddle point as opposed to a maximum indicates that it is an anticrossing, showing that there are strong interactions between electrons in these levels. The nature of the resulting ground states⁴ and excitations are however left as a subject of future study.

With V_{bg} increased still further such that negative values of V_{fg} are required to achieve filling factors below 8, all resistance minima become shallower. Beyond the anticrossing, the mobility gaps at $\nu=5$ and 7 correspond to spin-splitting gaps between levels of like cyclotron and valley indices and should remain constant, so long as the effective g factor remains constant and the valley splitting does not become large enough for levels of differing cyclotron indices to coincide. In the data shown, we interpret the minima becoming shallower as due to the increase in disorder^{14,15} as the wave function is pressed against the rougher Si/BOX interface.

As described earlier, for negative values of V_{bg} and positive V_{fg} all three samples show similar behavior corresponding to the wave function being pressed against the silicon-thermal-oxide interface. Similarly, for negative values of V_{fg} and positive V_{bg} the behavior among the samples is relatively similar corresponding to the wave function being pressed against the BOX-silicon interface, and the valley splitting is larger than the spin splitting in each sample. For the 25 nm wide sample [Fig. 2(c)], when positive voltages are applied to both the front and back gates, vertical and horizontal lines can be seen corresponding to two independent sets of Shubnikov-de Haas oscillations. There are two independent two-dimensional electron gasses with differing valley splitting in each layer. The 10 nm wide quantum well

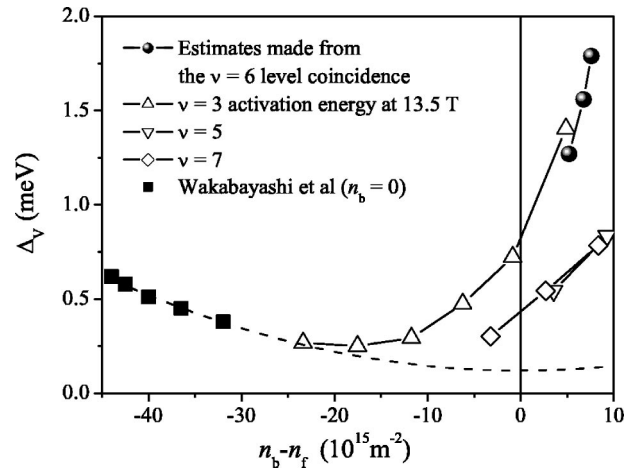


FIG. 4. The valley gap for the 8 nm wide sample plotted as a function of $n_b - n_f$ as defined in the body text. The circles show values estimated from the level coincidence at $\nu=6$ assuming a g factor of 2. The open symbols show the activation energies at a magnetic field of 13.5 T. The upward and downward triangles and diamonds represent values at filling factors 3, 5, and 7, respectively. The solid squares are taken from Ref. 17. The dashed line is a guide to the eye and represents qualitative behavior expected from a symmetric system (not a calculation).

[Fig. 2(b)] on the other hand shows a continuous evolution of the $\nu=4$ quantum Hall state from one end of the plot to the other rather like the 8 nm wide sample. However, at higher filling factors, features can be seen corresponding to the occupation of a second subband, broadly consistent with self-consistent calculations.¹⁶

We return our attention to the 8 nm wide sample and describe more quantitative aspects of the valley splitting. In the simple picture of the Landau levels presented in Fig. 3, the level coincidence at $\nu=6$ occurs under the condition: $\Delta_v = g^* \mu_B B$. Assuming a constant value for the g factor of 2, and taking the saddle point in $R_{xx}(V_{bg}, V_{fg})$ to correspond to the coincidence, we can make estimates of the valley splitting. The circular points in Fig. 4 show data-points obtained at 11, 13.5, and 15.5 T. The data points are plotted as a function of $n_b - n_f$, where n_f and n_b are electron concentrations supplied by the front and back gates, respectively and represents the degree of electrostatic asymmetry present in the system.

We have also made temperature-dependence measurements at odd filling factors and fitted the activated temperature range to $\sigma_{xx} = \sigma_0 \exp(-\Delta/2k_B T)$. The open data points in Fig. 4 show the extracted values for Δ . The values of energy gaps obtained in this way are strongly influenced by disorder and many-body effects^{14,15} and is therefore not a straightforward reflection of the bare valley splitting. This is confirmed by our magnetic-field dependence measurements of the activation energies which show that while the gaps at $\nu=5$ and 7 are essentially field independent, the gap at $\nu=3$ is strongly field enhanced, consistent with recent findings by Khrapai *et al.*³ It is also evident on inspecting Fig. 2(a) that the behavior associated with the lowest Landau level ($n=0$) is qualitatively different to that of the higher levels. This is expected to be due to strong electron-electron

interactions but its details are beyond the scope of this paper. What is clear from the data in Fig. 4, however, is that Δ is strongly asymmetric with respect to $n_b - n_f$. The changing valley splitting is due to the differences in the two Si/SiO₂ interfaces present in the system.

The activation gap for $\nu=3$ at large negative values of $n_b - n_f$ remains measurably large and even shows a slight increase beyond $n_b - n_f = -17 \times 10^{15} \text{ m}^{-2}$. We interpret this upturn to be of the same origin as the effect found in conventional MOSFET's. Values found by Wakabayashi *et al.*¹⁷ in a conventional silicon MOSFET are shown for comparison (no substrate bias is applied and n_b is set to zero). These values are obtained at very high filling factors by finding conditions where $2\Delta_V = g\mu_B B$ under tilted magnetic field⁷ and are expected to be relatively free of many-body effects compared with our activation measurements. The dashed line is a guide to the eye and shows the expected qualitative behavior where Δ_V has a finite value at $n_b - n_f = 0$ due to the residual confinement in the case of our quantum well.¹³ With $n_b - n_f$ made more negative, the wave function is increasingly confined to the thermally grown interface region and the valley splitting increases. This effect can also be observed in the 10 nm wide well [Fig. 2(b)]. At $V_{bg} = 0$ V, resistance minima at $\nu=5$ and 7 can hardly be observed. However, they evolve with decreasing V_{bg} and by -7 V, they can clearly be resolved on the gray-scale plot.

The result that the valley splitting is strongly enhanced by the Si/BOX interface is qualitatively consistent with conclu-

sions drawn from experiments on ultranarrow wells by Ouisse *et al.*¹³. It is likely that the extremely large values they observe are due to a combination of the strong confinement itself and the effect of the Si/BOX interface being enhanced due to the confinement.

Since the samples are heat treated for a prolonged period of time close to the melting point of silicon, one might expect the two Si/SiO₂ interfaces to be microscopically similar. However, AFM studies have shown that Si/BOX interfaces are not quite as smooth as their thermally grown counterpart¹¹ and that there are topological differences in the atomic terracing between the two interfaces.¹⁸ However, it is unknown how these microscopic differences lead to the observed differences in the valley splitting presented here. Theoretically predicted values of the valley splitting can strongly depend on the interface model used.^{1,19-21} Since our system shows reproducible differences at the two interfaces it should be possible to test models of the Si/SiO₂ interface.

To conclude, we have shown that the SIMOX MOSFET offers a new type of control over the valley splitting. The range over which it can be tuned is sufficient to observe level coincidences between levels of opposite spin and opposite valleys deep in the quantized Hall regime, and we have used this to obtain estimates of the valley splitting. We expect that our findings will allow much desired valley-resolved measurements of level coincidences between levels of different spin and cyclotron indices where spectacular effects have been observed recently in various systems.^{5,6}

*Present address: Department of Electrical and Electronic Engineering, Faculty of Engineering and Resource Science, Akita University, 1-1 Tegata Gakuen-machi, Akita-shi 010-8502, Japan.

¹T. Ando, A.B. Fowler, and F. Stern, *Rev. Mod. Phys.* **54**, 437 (1982).

²Y.P. Shkolnikov, E.P. De Poortere, E. Tutuc, and M. Shayegan, *Phys. Rev. Lett.* **89**, 226805 (2002).

³V.S. Khrapai, A.A. Shashkin, and V.T. Dolgoplov, *Phys. Rev. B* **67**, 113305 (2003)

⁴T. Jungwirth and A.H. MacDonald, *Phys. Rev. B* **63**, 035305 (2000)

⁵E.P. De Poortere, E. Tutuc, S.J. Papadakis, and M. Shayegan, *Science* **290**, 1546 (2000); J. Jaroszynski, T. Kndrearczyk, G. Karczewski, J. Wróbel, T. Wojtowicz, E. Papis, E. Kaminska, A. Piotrowska, D. Popović, and T. Dieti, *Phys. Rev. Lett.* **89**, 266802 (2002); S. Koch, J. Haug, K.V. Kitizing, and M. Razeghi, *Phys. Rev. B* **47**, 4048 (1993); K. Muraki T. Saku, and Y. Hirayama, *Phys. Rev. Lett.* **87**, 196801 (2001).

⁶U. Zeitler, H.W. Schumacher, A.G.M. Jansen, and R.J. Haug, *Phys. Rev. Lett.* **86**, 866 (2001).

⁷R.J. Nicholas, K. von Klitzing, and Th. Englert, *Solid State Commun.* **34**, 51 (1980).

⁸R.J. Nicholas, E. Kress-Rogers, F. Kuchar, M. Pepper, J.C. Portal, and R.A. Stradling, *Surf. Sci.* **98**, 283 (1980).

⁹K. Izumi, M. Doken, and H. Ariyoshi, *Electron. Lett.* **14**, 593 (1978).

¹⁰T. Ishiyama and M. Nagase, *Jpn. J. Appl. Phys., Part 1* **34**, 6019 (1995).

¹¹Y. Takahashi, A. Fujiwara, M. Nagase, H. Namatsu, K. Kurihara, K. Iwate, and K. Murase, *Int. J. Electron.* **86**, 605 (1999).

¹²T. Ouisse, S. Cristoloveanu, and D.K. Maude, *J. Appl. Phys.* **74**, 408 (1993).

¹³T. Ouisse, D.K. Maude, S. Horiguchi, Y. Ono, Y. Takahashi, K. Murase, and S. Christoleanu, *Physica B* **249-251**, 731 (1998).

¹⁴T. Ando and Y. Uemura, *J. Phys. Soc. Jpn.* **37**, 1044 (1974).

¹⁵A. Usher, R.J. Nicholas, J.J. Harris, and C.T. Foxon, *Phys. Rev. B* **41**, 1129 (1990).

¹⁶T. Ouisse, *J. Appl. Phys.* **76**, 5989 (1994).

¹⁷J. Wakabayashi, S. Kimura, Y. Koike, and S. Kawaji, *Surf. Sci.* **170**, 359 (1986), see also data by Kawaji *et al.*, in Ref. 1, p. 573.

¹⁸M. Nagase, T. Ishiyama, and K. Murase, in *Proceedings of the Sixth International Symposium on SOI Technology and Devices*, edited by S. Cristoloveanu (The Electrochemical Society, Pennington, NJ, 1994), p. 191.

¹⁹T. Ando, *Phys. Rev. B* **19**, 3089 (1979).

²⁰L.J. Sham and M. Nakayama, *Phys. Rev. B* **20**, 734 (1979).

²¹M. Nakayama, *Surf. Sci.* **98**, 358 (1980).